

Investigation of mechanisms of vacancy generation in silicon in the presence of a TiSi₂ film

S. B. Herner^{a)} and K. S. Jones

Department of Materials Science and Engineering, University of Florida, Gainesville, Florida 32611

H.-J. Gossmann, R. T. Tung, and J. M. Poate^{b)}

Bell Laboratories, Lucent Technologies, Murray Hill, New Jersey 07974

H. S. Luftman^{c)}

Bell Laboratories, Lucent Technologies, Breinigsville, Pennsylvania 18031

(Received 13 February 1997; accepted for publication 16 April 1997)

We have determined the perturbation in the silicon vacancy concentration induced by the presence of TiSi₂ films. Antimony in silicon doping superlattices was employed as a vacancy detector. Under all conditions studied (deposited titanium thickness 4–312 nm, 800–850 °C, 15–600 min), we always observe a relative vacancy supersaturation on the order of 1.5. Two mechanisms of vacancy injection during titanium silicidation were studied: (1) stress compensation; by varying the thickness of the deposited films and annealing for 60 min at 850 °C, a range of stresses was induced in the substrate via the coefficient of thermal expansion mismatch between the film and substrate. The observed vacancy supersaturation was independent of film thickness, indicating that stress compensation is not a mechanism of vacancy generation for titanium disilicide; (2) volume contraction; annealing for 15, 60, and 600 min at 800 °C after identical 30-nm-thick titanium films were deposited allowed the time variation of the vacancy supersaturation to be studied. While the vacancy supersaturation decayed slightly with time, its time dependence is incompatible with a large “pulse” of vacancies injected during the silicidation reaction. This indicates that volume contraction at the growing film interface is not a mechanism for vacancy generation. The thicker TiSi₂ films (>22 nm) and those annealed for ≤60 min were continuous in their coverage of the substrate as observed by transmission electron microscopy, while the thinner films and those annealed for longer times had islanded. However, there was no relationship between film coverage and vacancy behavior in the substrate, or was there any relation between deposition method (evaporation versus sputtering) and vacancy behavior. © 1997 American Institute of Physics. [S0021-8979(97)04814-7]

I. INTRODUCTION

Thin films utilized in silicon integrated circuit (IC) fabrication can perturb the native point defect equilibrium in the underlying substrate.^{1,2} The native point defect concentration in silicon plays a dominant role in the diffusion of common substitutional dopants and so changes from equilibrium are of obvious interest. Nevertheless, a proven mechanism of how a thin film effects a change in the native point defect concentration of the underlying substrates is still absent despite several theories. Several proposed mechanisms for native point defect generation in silicon with thermally grown silicon dioxide film and one for silicon nitride films are reviewed by Fahey, Griffin, and Plummer.³ Osada *et al.*⁴ have reported that increased silicon nitride film thickness has resulted in increased native point defect generation. They argued that the larger stress imposed by the thicker films was responsible for the observed native point defect behavior. Wen *et al.*⁵ proposed that the diffusing species during the

reaction of titanium with silicon to form titanium disilicide (TiSi₂) was the mechanism for the observed vacancy supersaturation in the silicon substrate. However, we have recently shown that this cannot explain the vacancy injection in silicon with a TiSi₂ film.⁶ Titanium disilicide films are used as ohmic contacts to highly doped silicon substrates in ICs. Contacts are typically formed by depositing titanium on silicon and annealing at elevated temperatures (>650 °C) to react the elements and form TiSi₂. It has been established that TiSi₂ films result in a relative vacancy supersaturation ($\sim 1.5 \times C_V^*$) and an interstitial undersaturation ($\sim 0.3 \times C_I^*$) in the underlying silicon, where C_V is the concentration of vacancies, C_I that of interstitials, and the asterisk denotes equilibrium.² It is unclear how this is accomplished. In this paper, we apply the reasoning of Osada *et al.* to vacancy generation in silicon with a TiSi₂ film. Like silicon nitride, TiSi₂ is under a tensile stress during annealing and results in a vacancy supersaturation in the silicon substrate. Another mechanism, volume contraction arising from the differing volumes of film and elemental precursors to the film, is also studied.^{7,8} This mechanism leads to a time dependence of the vacancy supersaturation. In addition to these two possible mechanisms of vacancy generation in silicon with a TiSi₂ film, we address the influence of film coverage and film deposition on the observed vacancy perturbation.

^{a)}Current address: Bell Laboratories, Lucent Technologies, Murray Hill, NJ 07974. Electronic mail: bherner@physics.bell-labs.com

^{b)}Current address: College of Arts and Sciences, New Jersey Institute of Technology, Newark, NJ 07102.

^{c)}Current address: Bell Laboratories, Lucent Technologies, Reading, PA 18103.

TABLE I. List of samples and annealing conditions. For the stress compensation study, three DSL samples had titanium (99.995% purity) evaporated by electron beam to area densities of 1.3, 2.3, and $3.4 \times 10^{17} \text{ cm}^{-2}$, as determined by Rutherford backscattering spectrometry (RBS). As the reaction of Ti and Si would consume the doping spikes in the growing TiSi_2 film for very thick films, titanium and silicon were coevaporated to a thickness of $\sim 680 \text{ nm}$ and an approximate composition of $\text{TiSi}_{1.8}$ (as deposited) on a fourth sample (*), again as determined by RBS. A thin film approximately 8 nm in thickness and compensation $\text{TiSi}_{1.8}$ was codeposited on a fifth sample (*). A rule-of-mixtures assumption of the silicon (only) and titanium (only) crystal structures yields titanium thicknesses of 312 and 4 nm for the two codeposited samples.

Sb concentration (cm^{-3})	Ti thickness (nm)	Deposition method	Anneal (in argon)
Stress compensation study			
6×10^{19}	4*	Evaporation	850 °C/60 min
1×10^{20}	22	Evaporation	850 °C/60 min
1×10^{20}	40	Evaporation	850 °C/60 min
1×10^{20}	59	Evaporation	850 °C/60 min
6×10^{19}	312*	Evaporation	850 °C/60 min
1×10^{20}	None (control)	None	850 °C/60 min
6×10^{19}	None (control)	None	850 °C/60 min
Volume contraction study			
6×10^{19}	30	Sputter	800 °C/15 min
6×10^{19}	30	Sputter	800 °C/60 min
6×10^{19}	30	Sputter	800 °C/600 min
6×10^{19}	None (control)	None	800 °C/15 min
6×10^{19}	None (control)	None	800 °C/60 min
6×10^{19}	None (control)	None	800 °C/600 min

II. EXPERIMENTAL DETAILS

We use the method of diffusion in dopant marker layers to study the concentration of native point defects in silicon. It has been shown that antimony diffuses by a vacancy-assisted mechanism.⁹ The diffusivity of antimony is therefore proportional to the concentration of silicon vacancies. The measurement of antimony diffusivity in doping superlattices (DSLs) represents a sensitive technique that provides depth profiles of vacancies.¹⁰

DSLs consisting of six antimony doping spikes of 10 nm width and spaced 100 nm apart were grown by low temperature-molecular beam epitaxy (LT-MBE) on float-zone silicon (100) wafers.¹¹ The shallowest spike is capped with 50 nm of silicon. DSLs with spike concentrations of 6×10^{19} or $1 \times 10^{20} \text{ cm}^{-3}$, respectively, were used. Prior to film deposition, all samples were prepared by a modified RCA clean and dilute HF (1:20) dip. The samples for the stress compensation study were loaded into an ultrahigh vacuum MBE chamber that was pumped down to a base pressure of 1×10^{-10} Torr and had titanium or titanium+silicon deposited by electron beam evaporation. The samples for the volume contraction study had 30 nm of titanium deposited by sputtering. The samples were subjected to various furnace anneals the specifics of which are listed in Table I. Anneals were done in argon of 99.995% purity flowing at a rate of 1500 sccm. The temperature accuracy was estimated to be ± 10 °C.

Film morphology was determined by transmission electron microscopy (TEM), composition by sputtering Auger electron spectroscopy (AES), and dopant concentration pro-

TABLE II. Comparison of antimony diffusivities in the DSL samples vs. a literature value.

850 °C/1 h anneal in argon	R.B. Fair ^a	Sb DSL ($6 \times 10^{19} \text{ cm}^{-3}$)	Sb DSL ($1 \times 10^{20} \text{ cm}^{-3}$)
$D_{\text{Sb}}^{\text{int}} (\text{cm}^2 \text{ s}^{-1})$	1.65×10^{-17}	$(2.20 \pm 0.32) \times 10^{-17}$	$(2.44 \pm 0.45) \times 10^{-17}$

^aReference 14.

files were obtained by secondary ion mass spectrometry (SIMS). In preparation for dopant depth profiling, silicide films were removed by chemically etching in a dilute HF (1:4) solution for 6 min. Annealing under the conditions listed in Table I results in a rough TiSi_2/Si interface; hence, the resulting silicon surface after etching was smoothed by a chemo-mechanical polishing (CMP) technique to prevent depth profiling artifacts that arise from sputtering through a rough surface.¹² Etching and CMP resulted in the loss of the shallowest one or two antimony doping spikes. Dopant diffusivities were extracted by analyzing each dopant spike separately as described in Ref. 10. The diffusion equation was solved with the process simulator PROPHET, accounting for concentration and electric field effects, which results in $D_{\text{Sb}}^{\text{int}}$, the intrinsic diffusivity of Sb.¹³ Diffusion coefficients are of the form $D = D_x h(1 + \beta m/n_i)$, where m is the electron concentration, n_i is the intrinsic carrier concentration, h is a Fermi level-dependent factor, and $\beta = 70 \exp(-0.43 \text{ eV}/kT)$. The fitting algorithm returns D_x from which we calculate $D_{\text{int}} = D_x(1 + \beta)$. Errors in the diffusivities have been estimated using a Monte Carlo approach.¹³

Table II compares the extracted intrinsic diffusivities in the control samples of the two antimony DSLs with a literature value.¹⁴ Our reported diffusivity enhancements are obtained relative to diffusivities from control samples, rather than the calculated literature equilibrium value. The use of control samples in this study eliminates such systematic errors as annealing temperature and time variations. Nevertheless, these systematic errors, which also include SIMS error, must be considered when the equilibrium diffusivity of antimony in this study is compared to the antimony diffusivity from other studies. For example, a 10 °C error in the anneal temperature at 850 °C results in a 42% difference in the antimony diffusivity calculated from literature values.¹⁴ With these items in mind, the extracted intrinsic diffusivities in Table II show excellent agreement with each other as well as the literature value.

III. RESULTS AND DISCUSSION

A. Stress compensation mechanism

Silicon nitride films on silicon are in tension at elevated temperatures due to a coefficient of thermal expansion (cte) mismatch. The compressed substrate has a smaller lattice constant than at equilibrium. The previous report⁴ on stress-related vacancy generation with silicon nitride films on silicon postulated that silicon atoms jump into the silicon nitride film, creating silicon vacancies in the substrate. Thicker films have a greater stress, and the larger vacancy supersaturations coincided with thicker films in that study. Titanium disilicide

TABLE III. Deposition conditions and morphology of the stress compensation samples. The stress in the substrates with islanded films has been estimated based on continuous film coverage. The variable x is the depth in the substrate (an asterisk signifies estimated titanium film thickness from codeposited titanium+silicon).

Ti thickness (nm)	Deposition	Annealed morphology	Estimated σ_{sub} as a function of film thickness
4*	Ti+Si	Islanded	$\sigma_{\text{sub}}(x)$
22	Ti (only)	Islanded	$6\sigma_{\text{sub}}(x)$
40	Ti (only)	Continuous	$10\sigma_{\text{sub}}(x)$
59	Ti (only)	Continuous	$15\sigma_{\text{sub}}(x)$
312*	Ti+Si	Continuous	$78\sigma_{\text{sub}}(x)$

is also in tension due to the cte mismatch with the substrate, and causes a vacancy supersaturation in the substrate. The stress compensation mechanism in silicon with a TiSi_2 film is investigated by varying the thickness of TiSi_2 films on anti-mony DSLs and annealing for 60 min at 850 °C.

After annealing, the resulting TiSi_2 films were all C54 phase, as shown by electron diffraction on plan view TEM samples. A thin $\text{TiO}_x\text{N}_{1-x}$ film formed on top of some of the TiSi_2 films as shown by sputtering AES, and this film has been described previously.¹⁵ In the films that had such a bilayer, the $\text{TiO}_x\text{N}_{1-x}$ film was far thinner than the TiSi_2 film and its presence is inconsequential to the results. The thinnest film ($t_{\text{Ti}}=4$ nm) had silicon codeposited in order to prevent the formation of a significant $\text{TiO}_x\text{N}_{1-x}$ film. The thickest film ($t_{\text{Ti}}=312$ nm) had silicon codeposited so that the growth of the resulting TiSi_2 film would not consume the silicon containing the antimony doping spikes. It has been previously shown that the codeposition of titanium and silicon yields the same native point defect perturbation as the reaction of Ti with the substrate.⁶ Since the resulting films have rough interfaces, making accurate TiSi_2 film thickness measurements difficult, we shall quote initial titanium thickness before TiSi_2 formation for comparison purposes. Due to the varying film thickness, the TiSi_2 films imposed a range of stresses in the substrate during annealing. Growth of the film and continued postgrowth annealing results in wafer curvature with the film in tension.¹⁶ The thermal stress in the substrate can be estimated by:¹⁷

$$\sigma_{\text{sub}} = 6E_s \langle \epsilon_s \rangle \Delta \left(\zeta - \frac{1}{3} \right), \quad (1)$$

where σ_{sub} is the substrate stress, E_s is Young's modulus of the substrate, $\langle \epsilon_s \rangle$ is the substrate strain, Δ is the layer-to-substrate thickness ratio, $\zeta = r_s / t_s$, r_s is the distance from the backside of the substrate, and t_s is the thickness of the substrate. This assumes that the stress is linearly dependent on the temperature, as shown by Svilan *et al.*¹⁶ Stresses in the compressed region of the substrate are estimated as a multiple of film thickness in Table III from Eq. (1). The thickest film should impose on the substrate 78× the stress of the thinnest film. As shown in Fig. 1(a), the thinner films ($t_{\text{Ti}} < 22$ nm) have completely islanded. The islanding of TiSi_2 and its variation with thickness is a well-known grain boundary wetting phenomenon.¹⁸ This should lead to a lower overall stress compared to those films ($t_{\text{Ti}} > 22$ nm) that have

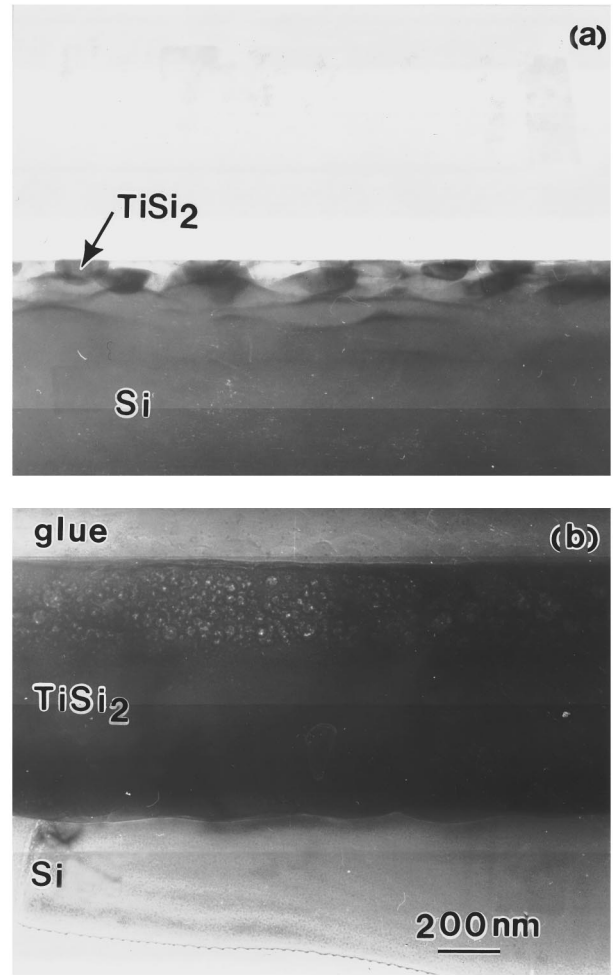


FIG. 1. Cross-sectional TEM micrographs of the annealed samples with (a) 4 nm titanium (as deposited), and (b) 312 nm titanium (as deposited). Samples were annealed for 60 min at 850 °C in argon.

continuous film coverage [Fig. 1(b)]. Nevertheless, we do not rule out a stressed region of the substrate in the neighborhood of each island.

A representative example of an antimony depth profile is shown in Fig. 2. The diffusivity of antimony is enhanced in the sample with a TiSi_2 film compared to the control sample, consistent with a vacancy supersaturation. The first doping spike in the TiSi_2 sample is lost due to etching and polishing. Figure 3 shows the normalized diffusivities of antimony with depth in the samples with a TiSi_2 film. There is no significant variation in antimony diffusivity with depth in the superlattice. The extracted normalized diffusivities are averaged over the depth and plotted against titanium thickness in Fig. 4. It is apparent from Fig. 4 that little variation is observed with film thickness. Clearly, a vacancy supersaturation that varies with the stress level in the substrate is not occurring in the samples with a TiSi_2 film.

Osada *et al.* observed boron diffusivity being increasingly retarded in silicon with thicker silicon nitride films.⁴ Since boron diffuses primarily by an interstitial mechanism,³ retarded boron diffusion was attributed to an interstitial depletion caused by interstitial-vacancy annihilation. The degree of interstitial undersaturation was reasoned to increase

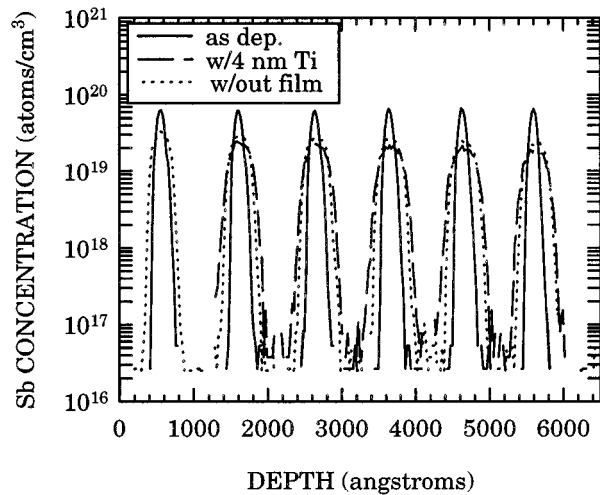


FIG. 2. Representative SIMS depth profiles of antimony doping superlattices. The samples have been annealed for 60 min at 850 °C.

with increasing vacancy supersaturation. Smaller boron diffusivities were therefore attributed to greater vacancy supersaturations. Estimates of the stress in silicon nitride and titanium disilicide films at elevated temperatures are similar.^{19,20} Since we do not see a similar effect as Osada *et al.* despite a similar range of film thickness and a more sensitive dopant marker technique, we rule out the mechanism of stress relief of the film in the near interface region in silicon with a TiSi₂ film.

Several other observations are pertinent to the data. That the diffusing species during silicide growth is not a factor in the change from point defect equilibrium is evident again in this data.⁶ There is no significant difference in antimony diffusivity in samples with TiSi₂ films formed from deposited titanium (only) versus codeposited titanium + silicon. The codeposited samples require little silicon diffusion from the

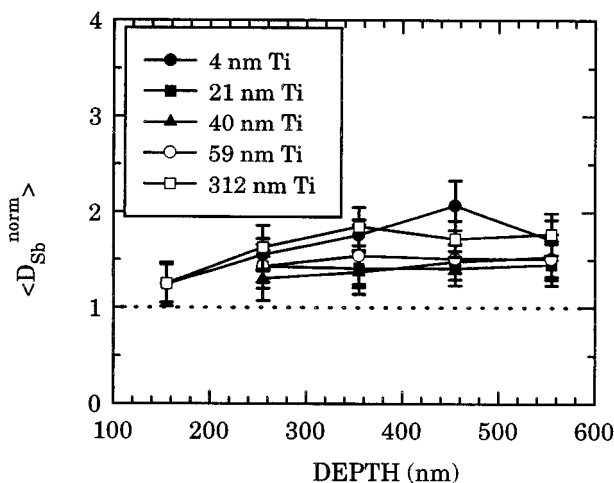


FIG. 3. Depth profiles of D_{Sb}^{norm} , where $D_{Sb}^{norm} = \langle D_{Sb}^{int, Ti film} \rangle / \langle D_{Sb}^{int, no film} \rangle$ in silicon with TiSi₂ films of varying thicknesses. Samples were annealed for 60 min at 850 °C.

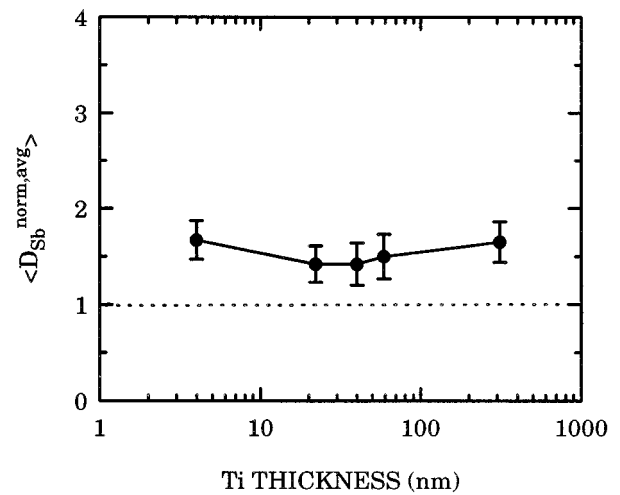


FIG. 4. Plot of D_{Sb}^{norm} vs titanium thickness (averaged over the depth). Samples were annealed for 60 min at 850 °C.

substrate relative to the samples with titanium (only) to form TiSi₂, and yet have the same relative vacancy supersaturation as the titanium (only) samples.

B. Volume contraction mechanism

The volume contraction mechanism is studied by varying the annealing time of antimony DSLs with TiSi₂ films of identical thickness. Since the growth of TiSi₂ at 800 °C is complete in less than 1 min,²¹ the vacancy perturbation should be large at short anneal times and decay to equilibrium with continued annealing if this mechanism is valid. The films in this study show a range of morphologies similar to the films with various thicknesses discussed in Sec. III A. The film annealed at 800 °C for 600 min has an island morphology, while the films with the shorter anneal times (15 and 60 min) are continuous, but with rough interfaces. The degree of islanding in the 600 min anneal sample is not as severe as that observed in the thinnest film in the stress compensation study [Fig. 1(a)]. Antimony diffusion behavior is also similar to that observed in the samples in Sec. III A, namely, diffusion is enhanced in samples with a TiSi₂ film. There is little depth dependence to the diffusivity (Fig. 5), similar to the results of Sec. III A. The larger error on the diffusivity estimate at 15 min reflects the small diffusion distance. The vacancy enhancement shows an apparent decay with time (Fig. 6). However, given the large error in the measurement of antimony diffusion in the 15 min sample, even this slight decay may not be real.

Tan and Gösele⁷ proposed that volume expansion at a growing silicon dioxide film interface is the mechanism for the interstitial supersaturation observed in the silicon substrate. The constituent elements were calculated to occupy less space than the silicon dioxide molecule, and the resulting expansion was thought to be accommodated by the generation of silicon interstitials. They noted, however, that silicon nitride films undergo a volume expansion as well, and yet result in a vacancy supersaturation in the substrate. A similar mechanism was proposed by Itayantsev and

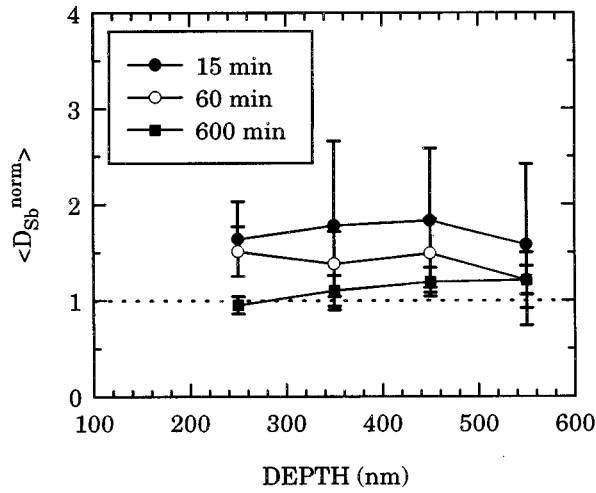


FIG. 5. Depth profiles of D_{Sb}^{norm} in the time variation samples. Samples were annealed at 850 °C with 30 nm of titanium.

Kuznetsov⁸ for vanadium disilicide (VSi_2) films on silicon. They reasoned that the volume contraction of VSi_2 is accommodated by vacancy generation. We can test this argument for $TiSi_2$ volume contraction and vacancy injection. The relative volume contraction in $TiSi_2$ formation is given by:

$$\Delta V = \frac{(V_{Ti} + 2V_{Si}) - V_{TiSi_2}}{(V_{Ti} + 2V_{Si})}, \quad (2)$$

resulting in a 23% volume contraction.¹⁹ A relatively large enhancement in $\langle C_V \rangle / C_V^*$ (a “pulse”) should then be observed at short annealing times, with a decay in this enhancement as the system returns to equilibrium with further annealing. If titanium disilicide growth and vacancy injection occur over an initial time period τ_E during the anneal, τ is the total annealing time, E is initial vacancy supersaturation during the initial time period τ_E , $D_{Sb}^{norm} = \langle D_{Sb}^{Ti} \rangle / D_{Sb}^*$, and assuming a vacancy diffusivity $D_V > (550 \text{ nm})^2 / 900 \text{ s} = 3.4 \times 10^{-12} \text{ cm}^2 \text{ s}^{-1}$, the relative vacancy concentration in the superlattice is:

$$\begin{aligned} \frac{\langle C_V \rangle}{C_V^*} &= D_{Sb}^{norm} = \frac{1}{\tau} \int_0^\tau \frac{C_V}{C_V^*} dt = \frac{1}{\tau} \left[\int_0^{\tau_E} E dt + \int_{\tau_E}^\tau dt \right] \\ &= \frac{\tau_E(E-1)}{\tau} + 1. \end{aligned} \quad (3)$$

By substituting the extracted D_{Sb}^{norm} value at $\tau=600$ min from the data, selecting $\tau_E=1$ min, representing a maximum time for film growth at 800 °C, and solving Eq. (3) yields $E=61$. Using this value for E for $\tau < 600$ min to solve Eq. (3) yields the dotted line in Fig. 6. It is apparent that the observed vacancy concentration is inconsistent with a pulse.

Two previous reports^{2,22} also indicate that the vacancy supersaturation in silicon with a $TiSi_2$ film is not the result of a pulse. When 30 nm of titanium is deposited on antimony DSLs and annealed for 60 min at 800 or 890 °C, extracted antimony diffusivities (normalized) indicate $\langle C_V \rangle / C_V^*$ values of 1.9 and 1.4, respectively, averaged over the extent of the DSL.² If the vacancies were injected as a pulse, $\langle C_V \rangle / C_V^*$ should be much larger at 800 than 890 °C, due to the smaller

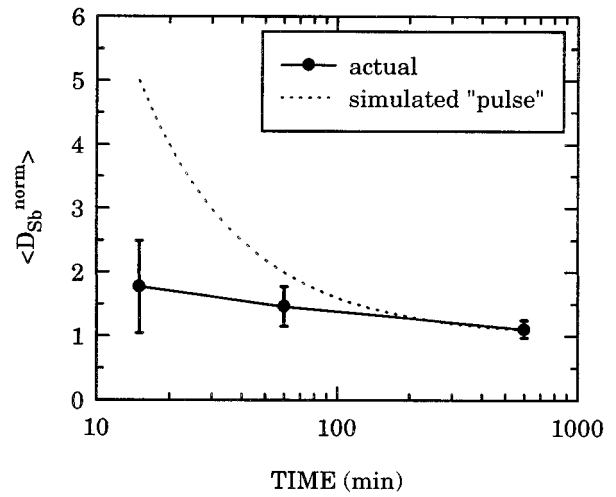


FIG. 6. Plot of D_{Sb}^{norm} vs time (averaged over the depth). Samples were annealed at 850 °C with 30 nm of titanium. The dashed line represents the expected profile of a pulse of vacancies.

$C_V^* [C_V^*(890 \text{ °C}) / C_V^*(800 \text{ °C} \sim 5)]$.²³ When silicon with a pre-existing layer of extrinsic dislocation loops is annealed with 30 nm of Ti, the loops dissolve at a faster rate than samples annealed without Ti.²² The enhanced loop dissolution was attributed to a vacancy supersaturation, with vacancies recombining with the interstitials in the loops. The enhanced loop dissolution was observed to be about monotonous with annealing time at 840 and 890 °C. These two studies as well as the present one indicate that the vacancy supersaturation is at least partially continuous with time, and does not occur as a single, finite pulse of vacancies.

Two other observations are pertinent with the results from Sec. III B. Sputter deposited atoms are more energetic than those deposited from evaporation, and can be expected to damage the substrate more, which could possibly influence point defect behavior. The diffusion results from the samples with titanium sputter deposited show little difference to the results from Sec. III A, in which titanium was deposited by evaporation. This indicates no real dependence on film deposition method. If the point defect perturbation were related to the area of the $TiSi_2/Si$ interface, a smaller perturbation would be observed in the samples with a thin $TiSi_2$ film (e.g., 4 nm titanium) than the thicker samples (e.g., 312 nm titanium). The thinner films have far smaller coverage of the substrate after the anneal is complete due to islanding than the thicker films (Fig. 1). Nevertheless, this does not affect the point defect behavior.

IV. CONCLUSION

Discovery of the mechanism(s) by which $TiSi_2$ films effect a change in the vacancy concentration in the underlying silicon substrate has so far proved elusive. In this report, we exclude stress compensation and volume contraction at the $TiSi_2/Si$ interface as mechanisms for vacancy generation in silicon with a $TiSi_2$ film. Silicon DSLs with deposited titanium ranging in thickness from 4 to 312 nm annealed for 60 min at 850 °C gives a $TiSi_2$ film and the same relative va-

cancy supersaturation ($\sim 1.5\times$) in the silicon substrate, ruling out stress compensation. Silicon DSLs with 30 nm of titanium annealed for times ranging from 15 to 600 min at 800 °C show an antimony diffusion behavior that is incompatible with a pulse of vacancies injected during film growth, ruling out volume contraction. The morphology of the annealed TiSi₂ films ranged from continuous coverage of the substrate to islanded, but no correlation between film shape and the observed vacancy behavior was observed, not did we observe any difference with the method of film deposition, namely evaporation versus sputtering.

ACKNOWLEDGMENTS

We thank T. Boone for expert substrate preparation, C. S. Rafferty for the provision of PROPHET and many useful discussions, N. Ibrahim for the Ti sputter depositions, and E. S. Lambers for the AES analysis. The work at the University of Florida was funded by the SEMATECH consortium. One of the authors (S.B.H.) thanks Bell Laboratories, Lucent Technologies for partial financial support.

- ¹P. A. Packan and J. D. Plummer, *J. Appl. Phys.* **68**, 4327 (1990); T. K. Mogi, H.-J. Gossmann, C. S. Rafferty, H. S. Luftman, F. C. Unterwald, T. Boone, M. O. Thompson, and J. M. Poate, *Mater. Res. Soc. Symp. Proc.* **355**, 157 (1995).
²S. B. Herner, K. S. Jones, H.-J. Gossmann, J. M. Poate, and H. S. Luftman, *Appl. Phys. Lett.* **68**, 1687 (1996).
³P. M. Fahey, P. B. Griffin, and J. D. Plummer, *Rev. Mod. Phys.* **61**, 289 (1989).
⁴K. Osada, Y. Zaitso, S. Matsumoto, M. Yoshida, E. Arai, and T. Abe, *J. Electrochem. Soc.* **142**, 202 (1995).

- ⁵D. S. Wen, P. L. Smith, C. M. Osburn, and G. A. Rozgonyi, *Appl. Phys. Lett.* **51**, 1182 (1987).
⁶S. B. Herner, K. S. Jones, H.-J. Gossmann, R. T. Tung, J. M. Poate, and H. S. Luftman, *Appl. Phys. Lett.* **68**, 2870 (1996).
⁷T. Y. Tan and U. Gösele, *Appl. Phys. Lett.* **39**, 96 (1981).
⁸A. G. Italyantsev and A. Y. Kuznetsov, *Appl. Surf. Sci.* **73**, 203 (1993).
⁹P. Fahey, G. Barbuscia, M. Moslehi, and R. W. Dutton, *Appl. Phys. Lett.* **46**, 784 (1985).
¹⁰H.-J. Gossmann, A. M. Vredenberg, C. S. Rafferty, H. S. Luftman, F. C. Unterwald, D. C. Jacobson, T. Boone, and J. M. Poate, *J. Appl. Phys.* **74**, 3159 (1993).
¹¹H.-J. Gossmann, F. C. Unterwald, and H. S. Luftman, *J. Appl. Phys.* **73**, 8237 (1993).
¹²S. B. Herner, B. P. Gila, K. S. Jones, H.-J. Gossmann, J. M. Poate, and H. S. Luftman, *J. Vac. Sci. Technol. B* **14**, 3593 (1996).
¹³M. R. Pinto, D. M. Boulton, C. S. Rafferty, R. K. Smith, W. M. Coughran, Jr., I. C. Kizilyali, and M. J. Thoma, *IEDM Tech. Dig.* **92**, 923 (1992).
¹⁴R. B. Fair, *Impurity Doping Processes in Silicon*, edited by F. F. Y. Wang (North-Holland, Amsterdam, 1981), Chap. 7.
¹⁵S. B. Herner, V. Krishnamoorthy, A. Naman, K. S. Jones, H.-J. Gossmann, and R. T. Tung, *Thin Solid Films* (to be published).
¹⁶V. Sivilan, J. M. E. Harper, C. C. Cabral, Jr., and L. A. Clevenger, *Mater. Res. Soc. Symp. Proc.* (to be published).
¹⁷J. Vilms and D. Kerps, *J. Appl. Phys.* **53**, 1536 (1982).
¹⁸K. Maex, *Mater. Sci. Eng. Rep.* **R11**, 53 (1993).
¹⁹S. P. Murarka, *Silicides for VLSI Applications* (Academic, New York, 1983).
²⁰S. T. Ahn, H. W. Kennel, J. D. Plummer, and W. A. Tiller, *J. Appl. Phys.* **64**, 4914 (1988).
²¹H. Jeon, C. A. Sukow, J. W. Honeycutt, G. A. Rozgonyi, and R. J. Nemanich, *J. Appl. Phys.* **71**, 4269 (1992); C. A. Pico and M. G. Legally, *ibid.* **64**, 4957 (1988).
²²S. B. Herner, V. Krishnamoorthy, and K. S. Jones, *Appl. Surf. Sci.* **103**, 378 (1996).
²³T. Y. Tan and U. Gösele, *Appl. Phys. A* **37**, 1 (1985).